Chapter 20:

The Representative Elements: Groups 5A Through 8A

20.1 The Group 5A Elements

TABLE 20.1 Selected Physical Properties, Sources, and Methods of Preparation for the Group 5A Elements

Element	Electro-negativity	Sources	Method of Preparation
Nitrogen	3.0	Air	Liquefaction of air
Phosphorus	2.1	Phosphate rock ($Ca_3(PO_4)_2$)	$2Ca_3(PO_4)_2 + 6SiO_2 \rightarrow 6CaSiO_3 + P_4O_{10}$
		Fluorapatite ($Ca_5(PO_4)_3F$)	$P_4O_{10} + 10C \rightarrow 4P + 10CO$
Arsenic	2.0	Arsenopyrite (Fe_3As_2, FeS)	Heating arsenopyrite in the absence of air
Antimony	1.9	Stibnite (Sb_2S_3)	Roasting Sb_2S_3 in air to form Sb_2O_3 and then reduction with carbon
Bismuth	1.9	Bismite (Bi_2O_3), bismuth glance (Bi_2S_3)	Roasting Bi_2S_3 in air to form Bi_2O_3 and then reduction with carbon

Figure 20.1: The molecules of the types MX_3, MX_5, and MX_6 formed by Group 5A elements.

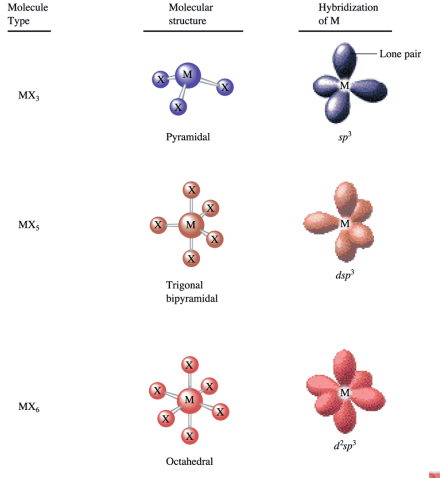

Figure 20.2: The structures of the tetrahedral MX_4^+ and octahedral MX_6^- ions.

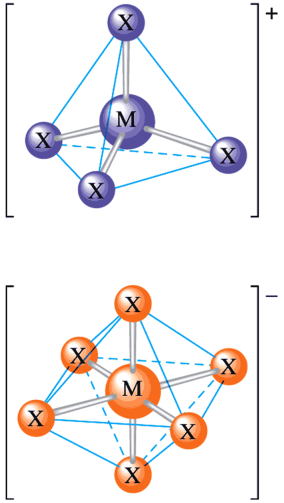

20.2 The Chemistry of Nitrogen

Nitrogen

The great stability of the N≡N bond means that most binary compounds containing nitrogen decompose exothermically to the elements

- $NO_2(g) \rightarrow {}^1/_2N_2(g) + O_2(g) \quad \Delta H° = -34$ kJ
- $N_2H_4(g) \rightarrow N_2(g) + 2H_2(g) \quad \Delta H° = -95$ kJ

Figure 20.3: An inert-atmosphere box used when working with oxygen- or water-sensitive materials.

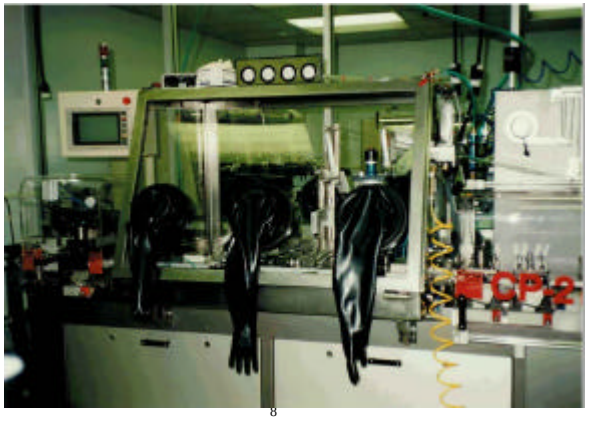

Figure 20.4: Chemical explosives are used to demolish a building in Miami, Florida.

Nitroglycerin

硝化甘油

Figure 20.5: A schematic diagram of the Haber process for the manufacture of ammonia.

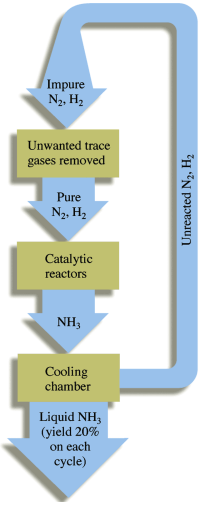

Nitrogen Fixation

- . . . the process of transforming N_2 to other nitrogen-containing compounds.

The Haber Process

$N_2(g) + 3H_2(g) \rightarrow 2NH_3(g) \quad \Delta H° = -92$ kJ

$P = 250$ atm

$T = 400°C$

Figure 20.6: The nitrogen cycle.

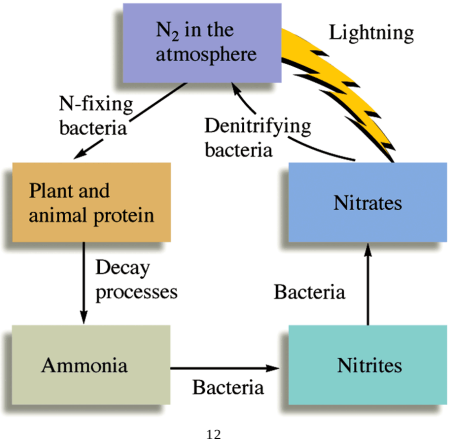

Nitrogen Hydrides

- Ammonia, NH_3
- Hydrazine, N_2H_4
- Monomethylhydrazine, $N_2H_3(CH_3)$

Blowing agents such as hydrazine, which forms nitrogen gas on decomposition, are used to produce porous plastics like these styrofoam products.

Figure 20.7: The molecular structure of hydrazine (N_2H_4).

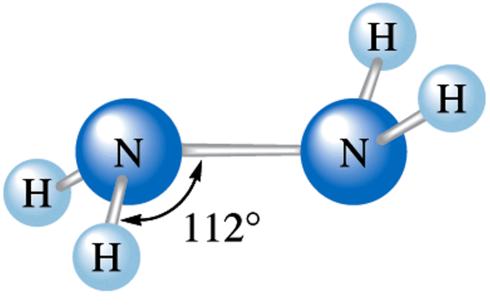

Nitrogen Oxides

Nitrogen in its oxides has an oxidation state from +1 to +5

Compound	Oxidation State of N
N_2O	+1
NO	+2
N_2O_3	+3
NO_2	+4
HNO_3	+5

TABLE 20.2 Some Common Nitrogen Compounds

Oxidation State of Nitrogen	Compound	Formula	Lewis Structure*
−3	Ammonia	NH_3	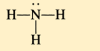
−2	Hydrazine	N_2H_4	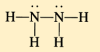
−1	Hydroxylamine	NH_2OH	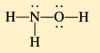
0	Nitrogen	N_2	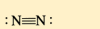
+1	Dinitrogen monoxide (nitrous oxide)	N_2O	
+2	Nitrogen monoxide (nitric oxide)	NO	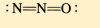
+3	Dinitrogen trioxide	N_2O_3	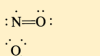
+4	Nitrogen dioxide	NO_2	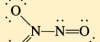
+5	Nitric acid	HNO_3	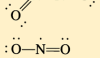

Figure 20.8: The molecular orbital energy-level diagram for nitric oxide (NO). The bond order is 2.5, or (8 – 3)/2.

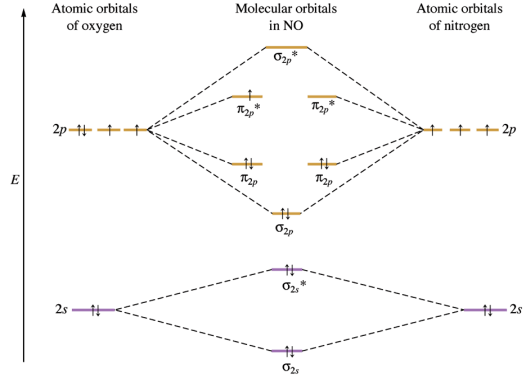

A copper penny reacts with nitric acid to produce NO gas, which is immediately oxidized in air to brown NO_2.

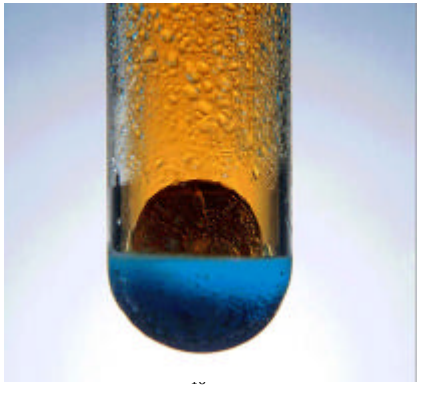

TABLE 20.3 Comparison of the Bond Lengths and Bond Energies for Nitric Oxide and the Nitrosyl Ion

	NO	NO^+
Bond length (pm)	115	109
Bond energy (kJ/mol)	630	1020
Bond order (predicted by MO model)	2.5	3

Figure 20.9: The Ostwald process.

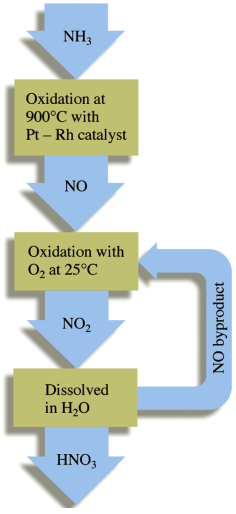

20.3 The Chemistry of Phosphorus

Figure 20.10: (a) The molecular structure of HNO_3. (b) The resonance structures of HNO_3.

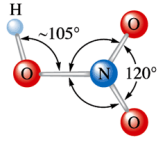

(a)

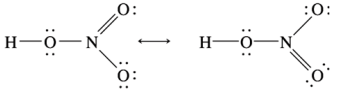

(b)

Allotropes of Phosphorus – P_4

- White Phosphorus (WP) = tetrahedral - very reactive
- Black Phosphorus (BP) = crystalline structure much less reactive
- Red Phosphorus (RP) = amorphous with P_4 chains.

$$\text{WP} \xrightarrow{\text{heat, 1 atm, no air}} \text{RP}$$

$$\text{WP or RP} \xrightarrow{\text{high pressure}} \text{BP}$$

Figure 20.11: (a) The P_4 molecule found in white phosphorus. (b) The crystalline network structure of black phosphorus. (c) The chain structure of red phosphorus.

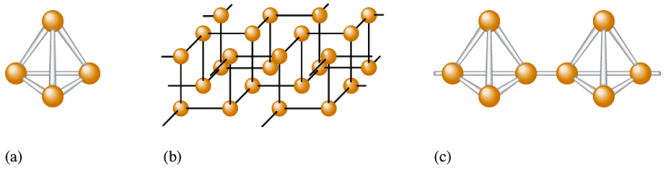

Fig. 20.13 (a) The structure of phosphorous acid (H_3PO_3). (b) The structure of hypophosphorous acid (H_3PO_2).

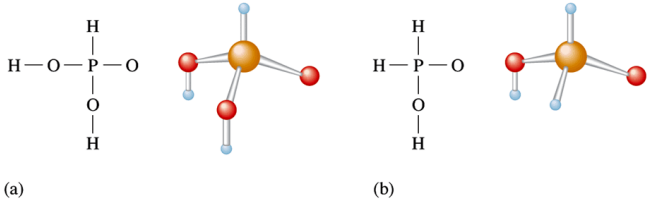

Figure 20.12: The structures of P_4O_6 and P_4O_{10}.

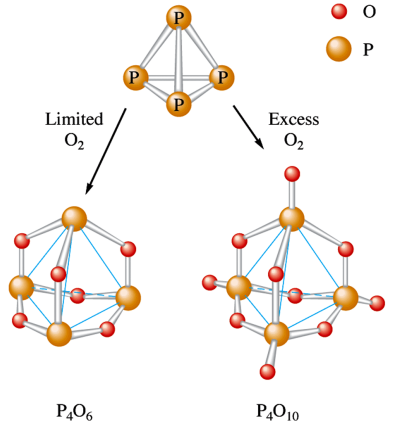

Figure 20.14: Structures of the phosphorus halides. (a) The PX_3 compounds have pyramidal molecules. (b) The gaseous and liquid phases of the PX_5 compounds are composed of trigonal bipyramidal molecules.

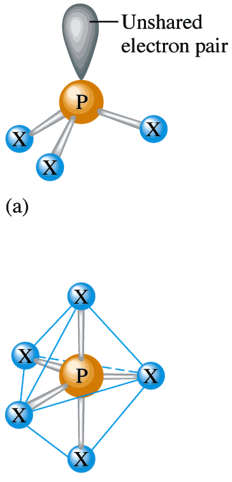

20.4 The Group 6A Elements

TABLE 20.4 Selected Physical Properties, Sources, and Methods of Preparation for the Group 6A Elements

Element	Electro-negativity	Radius of X^{2-} (pm)	Source	Method of Preparation
Oxygen	3.5	140	Air	Distillation from liquid air
Sulfur	2.5	184	Sulfur deposits	Melted with hot water and pumped to the surface
Selenium	2.4	198	Impurity in sulfide ores	Reduction of H_2SeO_4 with SO_2
Tellurium	2.1	221	Nagyagite (mixed sulfide and telluride)	Reduction of ore with SO_2
Polonium	2.0	230	Pitchblende	

20.5 The Chemistry of Oxygen

Fig. 9.39: The MO energy-level diagrams, bond orders, bond energies, and bond lengths for the diatomic molecules B_2 ~ F_2. Note that for O_2 and F_2 the σ_{2p} orbital is lower in energy than the π_{2p} orbitals.

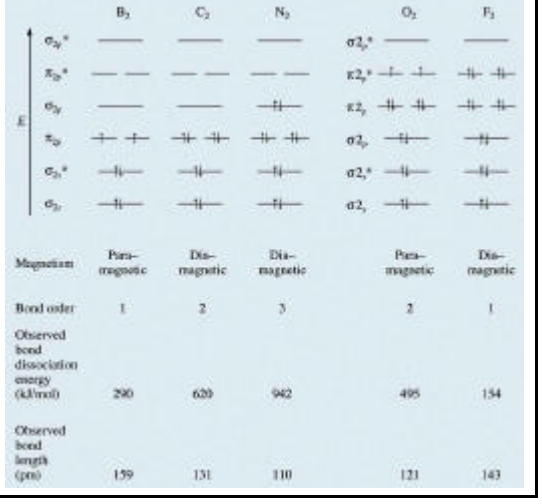

Figure 9.40: When liquid oxygen is poured into the space between the poles of a strong magnet, it remains there until it boils away. This attraction of liquid oxygen for the magnetic field demonstrates the paramagnetism of the O_2 molecule.

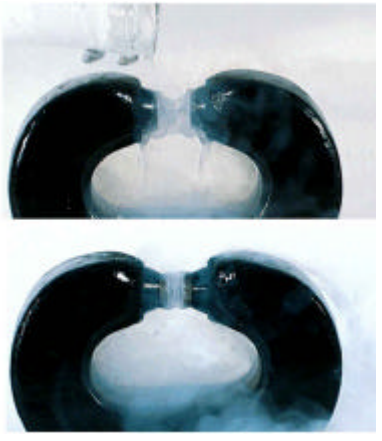

20.6 The Chemistry of Sulfur

Ozone

$3O_2(g) \leftrightarrow 2O_3(g) \qquad K \cong 10^{-57}$

Fig. 20.15: The Frasch process for recovering sulfur from underground deposits.

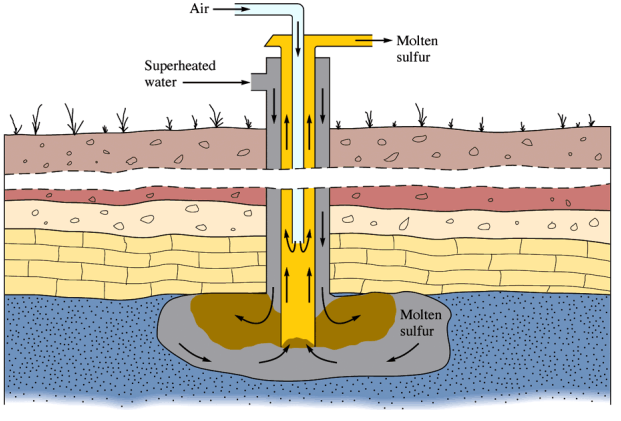

Figure 20.16: (a) The S_8 molecule. (b) Chains of sulfur atoms in viscous liquid sulfur. The chains may contain as many as 10,000 atoms.

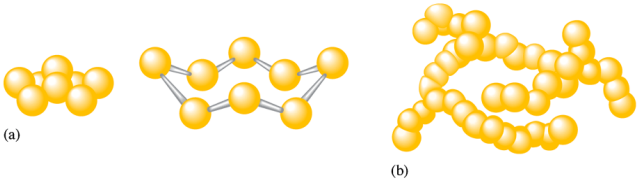

Pouring liquid sulfur into water to produce plastic sulfur.

Figure 20.17: (a) Crystals of rhombic sulfur. (b) Crystals of monoclinic sulfur.

Sulfur Oxide Reactions

- $2SO_2(g) + O_2(g) \rightarrow 2SO_3(g)$
- $SO_2(g) + H_2O(l) \rightarrow H_2SO_3(aq)$
- $SO_3(g) + H_2O(l) \rightarrow H_2SO_4(aq)$

Fig. 20.18: (a) Two of the resonance structures for SO_2. (b) SO_2 is a bent molecule with a 119-degree bond angle, as predicted by the VSEPR model.

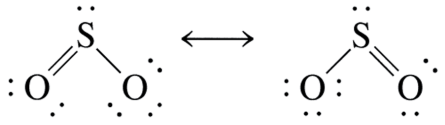

(a)

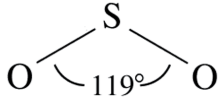

(b)

Figure 20.20: Different structures for solid SO_3. (a) S_3O_9 rings. (b) $(SO_3)_x$ chains. In both cases the sulfur atoms are surrounded by a tetrahedral arrangement of oxygen atoms.

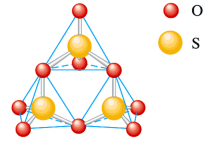

(a)

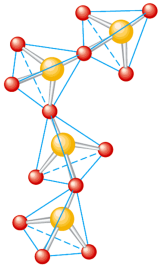

(b)

Figure 20.19: (a) Three of the resonance structures of SO_3. (b) A resonance structure with three double bonds. (c) SO_3 is a planar molecule with 120-degree bond angles.

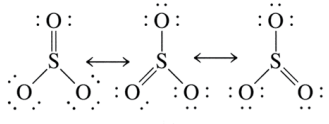

(a)

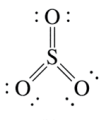

(b)

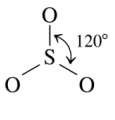

(c)

Figure 20.21: (a) A beaker of sucrose (table sugar). (b) Concentrated sulfuric acid reacts with the sucrose to produce a column of carbon (c), accompanied by an intense burnt-sugar odor.

TABLE 20.5 Common Compounds of Sulfur with Various Oxidation States

Oxidation State of Sulfur	Compounds
+6	SO_3, H_2SO_4, SO_4^{2-}, SF_6
+4	SO_2, HSO_3^-, SO_3^{2-}, SF_4
+2	SCl_2
0	S_8 and all other forms of elemental sulfur
−2	H_2S, S^{2-}

Figure 20.22: The structures of (a) SF_4, (b) SF_6, (c) S_2F_{10}, and (d) S_2Cl_2.

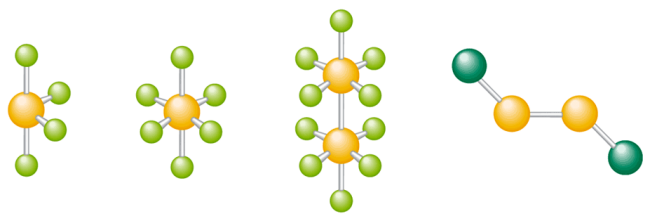

(a) (b) (c) (d)

20.7 The Group 7A Elements

TABLE 20.6 Trends in Selected Physical Properties of the Group 7A Elements

Element	Electro-negativity	Radius of X^- (pm)	$\mathscr{E}°$(V) for $X_2 + 2e \rightarrow 2X^-$	Bond Energy of X_2 (kJ/mol)
Fluorine	4.0	136	2.87	154
Chlorine	3.0	181	1.36	239
Bromine	2.8	185	1.09	193
Iodine	2.5	216	0.54	149
Astatine	2.2	—	—	—

TABLE 20.7 Some Physical Properties, Sources, and Methods of Preparation for the Group 7A Elements

Element	Color and State	Percentage of Earth's Crust	Melting Point (°C)	Boiling Point (°C)	Sources	Method of Preparation
Fluorine	Pale yellow gas	0.07	−220	−188	Fluorospar (CaF_2), cryolite (Na_3AlF_6), fluorapatite ($Ca_5(PO_4)_3F$)	Electrolysis of molten KHF_2
Chlorine	Yellow-green gas	0.14	−101	−34	Rock salt (NaCl), halite (NaCl), sylvite (KCl)	Electrolysis of aqueous NaCl
Bromine	Red-brown liquid	2.5×10^{-4}	−7.3	59	Seawater, brine wells	Oxidation of Br^- by Cl_2
Iodine	Violet-black solid	3×10^{-5}	113	184	Seaweed, brine wells	Oxidation of I^- by electrolysis or MnO_2

Preparation of Hydrogen Halides

$$H_2(g) + X_2(g) \rightarrow 2HX(g)$$

OR

Treating halide salts with acid:

$$CaF_2(s) + H_2SO_4(aq) \rightarrow CaSO_4(s) + 2HF(g)$$

$$2NaCl(s) + H_2SO_4(aq) \rightarrow Na_2SO_4(s) + 2HCl(g)$$

TABLE 20.8 Some Physical Properties of the Hydrogen Halides

HX	Melting Point (°C)	Boiling Point (°C)	H—X Bond Energy (kJ/mol)
HF	−83	20	565
HCl	−114	−85	427
HBr	−87	−67	363
HI	−51	−35	295

Figure 20.23: The hydrogen bonding among HF molecules in liquid hydrogen fluoride.

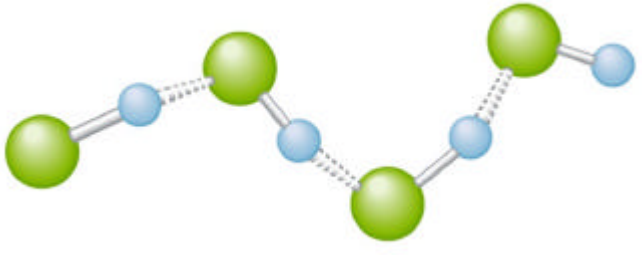

TABLE 20.9
The Enthalpies and Entropies of Hydration for the Halide Ions

$$X^-(g) \xrightarrow{H_2O} X^-(aq)$$

X^-	$\Delta H°$ (kJ/mol)	$\Delta S°$ (J/K · mol)
F^-	−510	−159
Cl^-	−366	− 96
Br^-	−334	− 81
I^-	−291	− 64

TABLE 20.10 The Known Oxyacids of the Halogens*

Oxidation State of Halogen	Fluorine	Chlorine	Bromine	Iodine*	General Name of Acids	General Name of Salts
+1	HOF	HOCl	HOBr	HOI	Hypohalous acid	Hypohalites, MOX
+3	**	$HOClO$	**	**	Halous acid	Halites, MXO_2
+5	**	$HOClO_2$	$HOBrO_2$	$HOIO_2$	Halic acid	Halates, MXO_3
+7	**	$HOClO_3$	$HOBrO_3$	$HOIO_3$	Perhalic acid	Perhalates, MXO_4

Figure 20.24: The structures of the oxychloro anions.

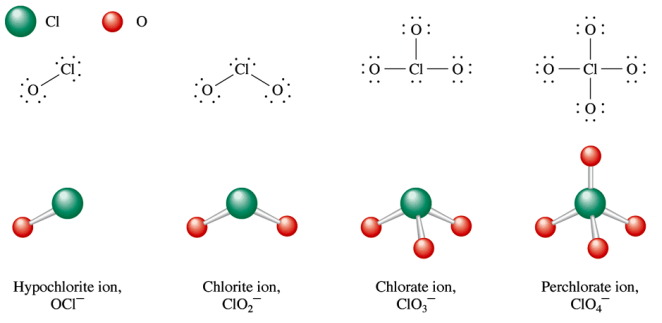

TABLE 20.11 Some Compounds of the Halogens with Nonmetals

Compounds with Group 3A Nonmetals	Compounds with Group 4A Nonmetals	Compounds with Group 5A Nonmetals	Compounds with Group 6A Nonmetals	Compounds with Group 7A Nonmetals
BX_3 (X = F,Cl,Br,I)	CX_4 (X = F,Cl,Br,I)	NX_3 (X = F,Cl,Br,I)	OF_2	ICl
BF_4^-		N_2F_4	O_2F_2	IBr
	SiF_4		OCl_2	BrF
	SiF_6^{2-}	PX_3 (X = F,Cl,Br,I)	OBr_2	BrCl
	$SiCl_4$	PF_5		ClF
		PCl_5	SF_2	
	GeF_4	PBr_5	SCl_2	ClF_3
	GeF_6^{2-}		S_2F_2	BrF_3
	$GeCl_4$	AsF_3	S_2Cl_2	ICl_3
		AsF_5	SF_4	IF_3
			SCl_4	
		SbF_3	SF_6	ClF_5
		SbF_5		BrF_5
			SeF_4	IF_5
			SeF_6	
			$SeCl_2$	IF_7
			$SeCl_4$	
			$SeBr_4$	
			TeF_4	
			TeF_6	
			$TeCl_4$	
			$TeBr_4$	
			TeI_4	

Figure 20.25: The idealized structures of the interhalogens ClF_3 and IF_5. In reality, the lone pairs cause the bond angles to be slightly less than 90°.

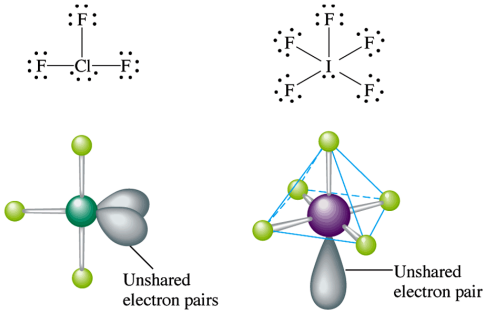

(a) ClF_3 is "T-shaped" (b) IF_5 is square pyramidal

變色眼鏡的原理

變色鏡(photochromic glass)使用在汽車車窗、太陽眼鏡、直觀顯示組件(visual display unit)上，它的基本組成是鹵素材質(如: AgCl+CuCl)

就像感光底片般，光感鏡片的顏色會變深是因為鏡片內含有銀及鹵素的化合物，如碘化銀。太陽光中的紫外線提供鹵素離子內含的些許電子足夠的能量做移動，這些電子會與銀離子結合以成為金屬銀的中性原子。這些銀原子之後便聚集成為微小顆粒，將光線散射掉而使鏡片顏色變深。

光照下： $Cl^- \rightarrow Cl + e^-$

$Ag^+ + e^- \rightarrow Ag$

上述過程是可逆的，一些太陽眼鏡遠離紫外線照射後數分鐘內就會恢復透明，而有些則必須透過加熱的過程才得以恢復原狀。在每個回復的過程中，電子從銀原子中脫離，造成其金屬簇再度分成銀離子。

不照光時： $Cl + Cu^+ \rightarrow Cl^- + Cu^{2+}$

$Cu^{2+} + Ag \rightarrow Cu^+ + Ag^+$

Ref: http://www.newton.com.tw/e-paper/epaper51.htm#01

照相與氧化還原的關係

$2Ag^+ + 2Br \xrightarrow{h\nu} 2Ag + Br_2$

底片感光活化

+developer 顯影劑 (hydroquinone)

將底片受光部分之AgBr還原為金屬Ag

照光顯像於感光相紙

+fixer 定影劑 (thiosulfate ions)

將未被還原之AgBr去除

洗去多餘的顯影劑 & 定影劑

製成負片

最後的相片成品

20.8 The Group 8A Elements

Noble Gases

- He, Ne and Ar form no compounds.

- Kr and Xe have been observed to form chemical compounds:

$Xe(g) + 2F_2(g) \rightarrow XeF_4(s)$ [6 atm, 400°C]

$XeF_6(s) + 3H_2O(l) \rightarrow XeO_3(aq) + 6HF(aq)$

Figure 20.26: The structures of several known xenon compounds

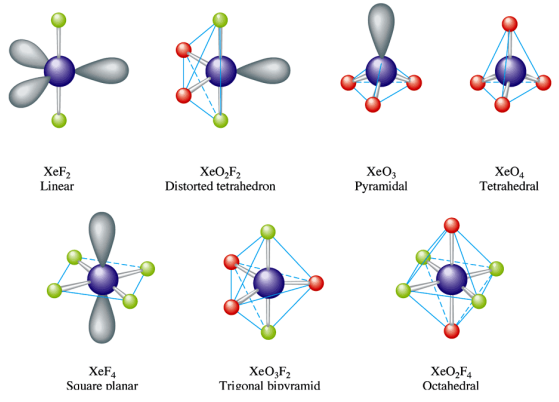

TABLE 20.12 Selected Properties of Group 8A Elements

Element	Melting Point (°C)	Boiling Point (°C)	Atmospheric Abundance (% by Volume)	Examples of Compounds
Helium	−270	−269	5×10^{-4}	None
Neon	−249	−246	1×10^{-3}	None
Argon	−189	−186	9×10^{-1}	None
Krypton	−157	−153	1×10^{-4}	KrF_2
Xenon	−112	−107	9×10^{-6}	XeF_4, XeO_3, XeF_6